Numerical analysis of Sakiadis flow problem considering Maxwell nanofluid

Meraj Mustafa [a, 1] and Junaid Ahmad Khan [b]

[a] *School of Natural Sciences (SNS), National University of Sciences and Technology (NUST), Islamabad 44000, Pakistan*

[b] *Research Centre for Modeling and Simulation (RCMS), National University of Sciences and Technology (NUST), Islamabad 44000, Pakistan*

Abstract: This article investigates the flow of Maxwell nanofluid over a moving plate in a calm fluid. Novel aspects of Brownian motion and thermophoresis are taken into consideration. Revised model for passive control of nanoparticle volume fraction at the plate is used in this study. The formulated differential system is solved numerically by employing shooting approach together with fourth-fifth-order-Runge-Kutta integration procedure and Newton's method. The solutions are greatly influenced with the variation of embedded parameters which include the local Deborah number De, the Brownian motion parameter Nb, the thermophoresis parameter Nt, the Prandtl number Pr and the Schmidt number Sc. We found that the variation in velocity distribution with an increase in local Deborah number De is non-monotonic. Moreover, the reduced Nusselt number has a linear and direct relationship with the local Deborah number De.

Keywords: Maxwell fluid; Moving plate; Nanoparticle; Brownian motion; Solar energy

1. Introduction

The study of nanofluid dynamics has been the subject of broad research community for the past few years mainly due to its promising applications in various industrial sectors. Researchers found that inclusion of nanometer sized metallic particles can markedly improve the transport properties of conventional coolants [1]. The scarcity of fossil fuels and environmental constraints have prompted researchers to explore the alternate sources of renewable energy such as solar energy. The energy obtained from nature can be optimally utilized by using nanoparticle working fluid [2]. It is seen that metallic nanoparticles in water-cooled nuclear reactor can produce significant economic gains as well as improved safety margins [3]. Nanofluids have also found relevance in various biomedical applications. For instance, magnetic nanofluids may be used to target drugs and radiation in cancer patients without affecting the healthy tissues [4]. In the literature two types of nanofluid models have been consistently used by the researchers namely the Tiwari and Das model [5] and the Buongiorno model [6]. The former focuses on the volume fraction of nanoparticles and later can be used to address the interesting aspects of Brownian motion and thermophoresis. Kuznetsov and Nield [7] used Buongiorno's model to investigate the natural convection from heated vertical plate embedded in nanofluid. Later, natural convective flow of nanofluid through a porous space was studied by Nield and Kuznetsov [8]. Flow of nanofluid over a moving flat plate in the presence of free stream velocity was described by Bachok et al. [9]. Khan and Pop [10] published a paper dealing with the flow of nanofluid above

[1]Corresponding author
E-mail address: meraj_mm@hotmail.com

a stretching extensible surface. Recently, significant numbers of studies pertaining to the flow and heat transfer in nanofluids have been reported [11-27].

Non-Newtonian fluid dynamics has been the subject of great concern to investigators presently. Most of the biological and industrial fluids such as polymers, paints, liquid detergents, multi-grade oils, greases, coolants, blood, printer inks etc. do not follow the classical Newton's law of viscosity and are termed as non-Newtonian. Researchers have proposed a variety of mathematical models to understand the dynamics of such fluids. For instance, the well known power-law model is able to predict the shear-thinning/thickening effects in the flow. Second grade fluid model is a visco-elastic model that can be used to understand the normal stress differences. On the other hand, Maxwell fluid is perhaps the most widely discussed viscoelastic fluid which has a tendency to describe the characteristics of fluid relaxation time. The boundary layer equations for two-dimensional flow of Maxwell fluids were first derived by Harris [28]. Sadeghly et al. [29] investigated the two-dimensional flow over a moving flat plate in quiescent ambient fluid utilizing Maxwell fluids. In another paper, Sadeghy et al. [30] analytically discussed the stagnation-point flow of Maxwell fluid. Mixed convection flow of Maxwell fluid under the influence of transverse magnetic field has been described by Kumari and Nath [31]. They found that an increase in the visco-elastic parameter corresponds to a reduction in the hydrodynamic boundary layer thickness. This outcome is qualitatively opposite to that of the visco-elastic parameter in second grade fluid. Hayat et al. [32] examined the stagnation-point flow of an electrically conducting Maxwell fluid over permeable stretching sheet. In recent years, various interesting boundary layer flow problems involving Maxwell fluid have been addressed (see [33-40]).

In this article, we discuss the classical Sakiadis flow problem by considering Maxwell Nanofluid. To our knowledge, the Sakiadis flow problem for viscoelastic fluids has never been considered before. Buongiorno's model together with the zero nanoparticle flux condition is followed in the problem formulation. Such consideration has industrial importance since many base fluids in realistic process exhibit viscoelastic properties. It has already been found that de-ionized water/poly-ethylene oxide as dispersant improves the convective transport of the fluid. Some examples of visco-elastic nanofluids are ethylene glycol/water-Al_2O_3, ethylene glycol/water-CuO and ethylene glycol/water-ZnO. Numerical simulations have been performed by the well known shooting approach. The role of pertinent parameters on the flow fields is thoroughly presented by plotting graphs.

2. Problem formulation

We consider the steady two-dimensional flow of an incompressible Maxwell nanofluid over a flat plate moving with the constant velocity U in its own plane (see Fig. 1). The plate is maintained at constant temperature T_w. The mass flux of nanoparticles from the plate is assumed to be zero. The ambient values of temperature and nanoparticle volume fraction are denoted by T_∞ and C_∞. The boundary layer equations governing the two-dimensional flow with heat and mass transfer in Maxwell fluid can be expressed as below (see Kuznetsov and Nield [7] and Harris [28]:

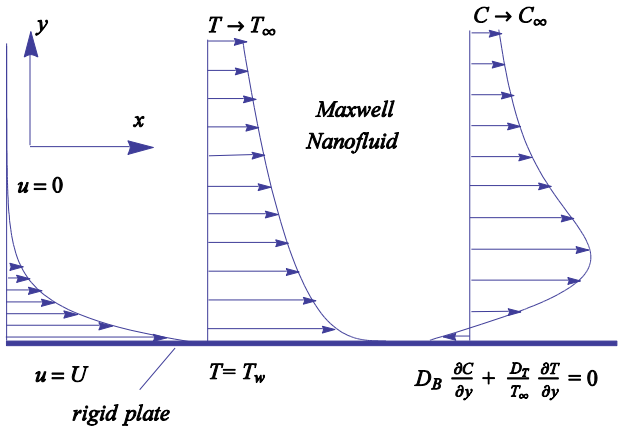

Fig. 1: Physical configuration and coordinate system.

$$\frac{\partial u}{\partial x}+\frac{\partial v}{\partial y}=0, \tag{1}$$

$$u\frac{\partial u}{\partial x}+v\frac{\partial u}{\partial y}+\lambda_1\left(u^2\frac{\partial^2 u}{\partial x^2}+v^2\frac{\partial^2 u}{\partial y^2}+2uv\frac{\partial^2 u}{\partial x\partial y}\right)=\nu_f\frac{\partial^2 u}{\partial y^2}, \tag{2}$$

$$u\frac{\partial T}{\partial x}+v\frac{\partial T}{\partial y}=\alpha_f\frac{\partial^2 T}{\partial y^2}+\tau\left[D_B\frac{\partial C}{\partial y}\frac{\partial T}{\partial y}+\frac{D_T}{T_\infty}\left(\frac{\partial T}{\partial y}\right)^2\right], \tag{3}$$

$$u\frac{\partial C}{\partial x}+v\frac{\partial C}{\partial y}=D_B\left(\frac{\partial^2 C}{\partial y^2}\right)+\frac{D_T}{T_\infty}\left(\frac{\partial^2 T}{\partial y^2}\right), \tag{4}$$

in which u and v are the velocity components along the $x-$ and $y-$directions respectively, ν_f is the kinematic viscosity, λ_1 is the relaxation time, T is the local fluid temperature, C is the local volume fraction of nanoparticles, α_f is the thermal diffusivity of the fluid, D_B is the Brownian diffusion coefficient, D_T is the thermophoretic diffusion coefficient, τ is the ratio of the effective heat capacity of the nanoparticle material to the effective heat capacity of the base fluid. The boundary conditions are

$$\begin{gathered} u=U,\quad v=0,\quad T=T_w,\quad D_B\frac{\partial C}{\partial y}+\frac{D_T}{T_\infty}\frac{\partial T}{\partial y}=0 \text{ at } y=0, \\ u\to 0,\quad T\to T_\infty,\quad C\to C_\infty \text{ as } y\to\infty. \end{gathered} \tag{5}$$

With an aid of following similarity transformations

$$\eta = \sqrt{\frac{U}{\nu_f x}}\, y, \quad u = Uf', \quad v = -\frac{1}{2}\sqrt{\frac{\nu_f U}{x}}\,(f - \eta f'),$$
$$\theta = \frac{T - T_\infty}{T_w - T_\infty}, \quad \phi = \frac{C - C_\infty}{C_\infty}, \tag{6}$$

Eq. (1) is identically satisfied and Eqs. (2)-(5) reduce to the following boundary value problem

$$De\left(2ff'f'' + \eta f'^2 f'' + f^2 f'''\right) - ff'' - 2f''' = 0, \tag{7}$$

$$\frac{1}{Pr}\theta'' + \frac{1}{2} f\theta' + Nb\theta'\phi' + Nt\theta'^2 = 0, \tag{8}$$

$$\phi'' + Sc\frac{1}{2} f\phi' + \frac{Nt}{Nb}\theta'' = 0, \tag{9}$$

$$f(0) = 0, \quad f'(0) = 1, \quad \theta(0) = 1, \quad Nb\phi'(0) + Nt\theta'(0) = 0,$$
$$f'(\infty) \to 0, \quad \theta(\infty) \to 0, \quad \phi(\infty) \to 0, \tag{10}$$

where prime denotes differentiation with respect to η, $De = \lambda_1 U / 2x$ is the local Deborah number, $Nb = \tau D_B C_\infty / \nu_f$ is the Brownian motion parameter, $Nt = \tau D_T (T_w - T_\infty) / T_\infty \nu_f$ is the thermophoresis parameter, $Pr = \nu_f / \alpha_f$ is the Prandtl number and $Sc = \nu_f / D_B$ is the Schmidt number.

The quantity of practical interest in this study is the local Nusselt number Nu_x, which is defined as

$$Nu_x = \frac{xq''}{k(T_w - T_\infty)}, \tag{11}$$

where $q'' = -k(\partial T / \partial y)|_{y=0}$ is a wall heat flux. Now using Eq. (6), Eq. (11) becomes

$$\mathrm{Re}_x^{-1/2}\, Nu_x = -\theta'(0) = Nur. \tag{12}$$

where $\mathrm{Re}_x = Ux/\nu$ is a local Reynolds number. Reduced Sherwood number which gives the mass transfer rate from the plate is now identically zero through the boundary conditions (10).

3. Numerical results and discussion

Eqs. (7)-(9) with the boundary conditions have been solved numerically through fourth-fifth-order-Runge-Kutta integration and Newton's method based shooting approach. The detailed procedure is explained in [23]. In addition the MATLAB built in function *bvp4c* is also used for computing the numerical solutions. The solutions obtained through both the methods are found in excellent agreement. For the case of pure viscous fluid with $\mathrm{Pr} = 0.7$, the values of $f''(0)$ and $\theta'(0)$ are 0.44375 and –0.34923 respectively which are in agreement with Cortell [41]. Tables

1 and 2 include the numerical results of reduced Nusselt number $-\theta'(0)$ for different values of the embedded parameters. The value of Prandtl number is chosen by keeping in view the thermophysical properties for Ethylene-glycol/water based nanofluids given in [43]. It is clear that $-\theta'(0)$ has a direct relationship with both the Prandtl number $\Pr$ and the local Deborah number De. On the other hand, it linearly decreases with an increase in the thermophoresis parameter Nt. In accordance with Kuznetsov and Nield [19], $\theta'(0)$ is negligibly affected by varying the Brownian motion parameter Nb.

Fig. 2 shows the velocity profiles for different values of local Deborah number De. The results of this Fig. are consistent with those of Sadeghy et al. [29]. Deborah number is defined as the fluid relaxation time to the fluid characteristic time scale. The velocity field f' slightly increases with an increase in De just close to the plate. However, it appears to decrease with an increase in De in the remaining portion of the boundary layer. The profiles tend to merge at shorter distances from the plate when De is incremented indicating that boundary layer thickness is a decreasing function of De. Physically, as De increases, the fluid strongly adheres to the boundary and hence creates a thinner boundary layer.

Fig. 3 is prepared to see the influence of Prandtl number $\Pr$ on the temperature distribution. Since $\Pr$ is inversely proportional to the thermal diffusivity, therefore, one anticipates that thermal boundary layer thickness would decrease upon increasing $\Pr$. It can be seen that slope of temperature θ near the wall is bigger for larger $\Pr$. Further, both temperature θ and thermal boundary layer thickness are found to decrease upon increasing the local Deborah number De.

In Fig. 4, temperature profiles are computed at various values of thermophoresis parameter. A stronger thermophoretic force allows nanoparticles of high thermal conductivity to enter deeper into the fluid and hence yields a thicker thermal boundary layer. The profiles exhibit similar pattern for any considered value of Nt in both Newtonian and visco-elastic nanofluids.

Nanoparticle volume fraction ϕ is plotted at different values of Schmidt number Sc in Fig. 5. Larger Schmidt number fluid has a weaker Brownian diffusion coefficient D_B and hence it produces shorter penetration depth for ϕ. ϕ appears to be negative near the plate, as also noticed by Kuznetsov and Nield [19]. Different from temperature θ, volume fraction of nanoparticles has direct relationship with the fluid relaxation time.

The variation in ϕ with an increase in Nt can be observed from Fig. 6. As effect of thermophoresis strengthens, the hot plate intensely blows the nanoparticles away from it and yields bigger penetration depth for ϕ. Whereas Fig. 7 indicates that ϕ is inversely proportional to the Brownian motion parameter Nb.

The reduced Nusselt number $-\theta'(0)$ as function of local Deborah number De is presented at different values of $\Pr$ and Nt in the Figs. 8 and 9 respectively. It is observed that $-\theta'(0)$ is directly as well as linearly proportional to the local Deborah number De in all the considered cases. We conclude that heat transfer rate decreases with an augmentation in thermophoretic force and this decrease is similar in magnitude for any considered local Deborah number De. The reduction in heat transfer rate occurs due to the fact that nanoparticles of high thermal conductivity are driven away from the plate towards the quiescent ambient fluid.

4. Concluding remarks

Model for two-dimensional flow of incompressible Maxwell nanofluid above a moving plate is presented and analyzed. The simulation assumes that the plate is kept at constant temperature and mass flux of nanoparticle is zero across it. Interesting aspects of Brownian motion and thermophoresis are considered. The numerical solution is achieved by shooting technique with fourth-fifth-order Runge Kutta integration procedure and Newton method. The key findings of this study are outlined as below.

1. Boundary layer thickness in visco-elastic nanofluid is shorter than that of the viscous nanofluid.
2. Reduced Nusselt number is directly proportional to the local Deborah number De.
3. Reduced Nusselt number has inverse relationship with the thermophoresis parameter and it is nearly independent of the Brownian motion parameter.
4. Schmidt number has a little impact on the temperature distribution whereas volume fraction of nanoparticles decreases when Sc is increased.
5. Local Deborah number De has dissimilar behaviors on temperature and nanoparticle volume fraction.
6. Influence of Brownian motion on local volume fraction of nanoparticles is qualitatively opposite to that of thermophoretic diffusion.
7. The case of Newtonian nanofluid which is not yet considered can be recovered from the presented model by choosing $De = 0$.

Appendix

The governing equation (2) is derived by Harris [42] while the energy and nanoparticle mass conservation equations for nanofluid flow are given by Buongiorno [6]. Here we present the outline of the derivation of these equations. The momentum equation for flow of upper-convected Maxwell fluid is given by [42]

$$\rho_f \frac{d\mathbf{V}}{dt} = \nabla \cdot \mathbf{S}, \tag{13}$$

where $\mathbf{V} = [u(x,y), v(x,y), 0]$ is the velocity field, ρ_f is the base fluid (Maxwell fluid) density, $d/dt \equiv \partial/\partial t + (\mathbf{V}\cdot\nabla)\mathbf{V}$ is the material time derivative and $\mathbf{S}$ is the extra stress tensor which obeys the following relationship:

$$\left(1 + \lambda_1 \frac{D}{Dt}\right)\mathbf{S} = \mu \mathbf{A_1}, \tag{14}$$

in which λ_1 is the fluid relaxation time, $\mathbf{A_1} = (\nabla\mathbf{V}) + (\nabla\mathbf{V})^t$ is the first Rivlin-Ericksen tensor and D/Dt is the convected time derivative. For any vector $\mathbf{A}$ we have [42]

$$\frac{D}{Dt}(A)_i = \frac{\partial}{\partial t}(A)_i + \mathbf{V}_j (A)_{i,j} - \mathbf{V}_{i,j} (A)_j, \tag{15}$$

after some manipulation in Eqs. (15) and (16) we arrive at the following.

$$\rho_f\left(1+\lambda_1\frac{D}{Dt}\right)\frac{d\mathbf{V}}{dt}=\mu\left(\nabla.\mathbf{A_1}\right), \tag{16}$$

Using Eq. (17) with $i=1$ one obtains

$$\frac{D}{Dt}\left(\frac{d\mathbf{V}}{dt}\right)_1=\frac{\partial}{\partial t}\left(\frac{d\mathbf{V}}{dt}\right)_1+(\mathbf{V})_1\left(\frac{d\mathbf{V}}{dt}\right)_{1,1}+(\mathbf{V})_2\left(\frac{d\mathbf{V}}{dt}\right)_{1,2}-(\mathbf{V})_{1,1}\left(\frac{d\mathbf{V}}{dt}\right)_1-(\mathbf{V})_{1,2}\left(\frac{d\mathbf{V}}{dt}\right)_2, \tag{17}$$

$$\left(\frac{d\mathbf{V}}{dt}\right)_1=\frac{du}{dt}=u\frac{\partial u}{\partial x}+v\frac{\partial u}{\partial y}, \tag{18}$$

$$\left(\frac{d\mathbf{V}}{dt}\right)_2=\frac{dv}{dt}=u\frac{\partial v}{\partial x}+v\frac{\partial v}{\partial y}, \tag{19}$$

substituting Eqs. (21) – (23) in (19) and using the continuity equation we obtain

$$u\frac{\partial u}{\partial x}+v\frac{\partial u}{\partial y}+\lambda_1\left(u^2\frac{\partial^2 u}{\partial x^2}+v^2\frac{\partial^2 u}{\partial y^2}+2uv\frac{\partial^2 u}{\partial x\partial y}\right)=\nu_f\left(\frac{\partial^2 u}{\partial x^2}+\frac{\partial^2 u}{\partial y^2}\right), \tag{20}$$

where ν_f is the kinematic viscosity of the base fluid. Similarly the $y-$ component of momentum Eq. (19) has the form

$$u\frac{\partial v}{\partial x}+v\frac{\partial v}{\partial y}+\lambda_1\left(u^2\frac{\partial^2 v}{\partial x^2}+v^2\frac{\partial^2 v}{\partial y^2}+2uv\frac{\partial^2 v}{\partial x\partial y}\right)=\nu_f\left(\frac{\partial^2 v}{\partial x^2}+\frac{\partial^2 v}{\partial y^2}\right). \tag{21}$$

Consider the incompressible flow of Maxwell fluid composed of nanometer-sized metallic particles. Energy equation in absence of viscous dissipation, Joule heating, heat source/sink and thermal radiation is given by

$$(\rho c)_f\left(\frac{\partial T}{\partial t}+\mathbf{V}.\nabla T\right)=-\nabla.\mathbf{q}+h_s\nabla.\mathbf{j}_s, \tag{22}$$

where $(\rho c)_f$ is the effective heat capacity of the base fluid, $\mathbf{q}$ is the heat flux, h_s is the specific enthalpy and $\mathbf{j}$ is the diffusive mass flux. Following Buongiorno [6] the heat flux $\mathbf{q}$ is given by

$$\mathbf{q}=-k\nabla T+h_s\mathbf{j}_s;\quad h_s=c_pT, \tag{23}$$

where k is the thermal conductivity. The diffusive mass flux due to Brownian motion and thermophoretic diffusion is given by

$$\mathbf{j}_s = \mathbf{j}_{s,B} + \mathbf{j}_{s,T} = -\rho_s D_B \nabla C - \rho_s D_T \frac{\nabla T}{T_\infty}, \tag{24}$$

in which D_B is the Brownian diffusion coefficient given by the Einstein–Stokes's equation, and D_T is the thermophoretic diffusion coefficient. Now substituting the expressions for $\mathbf{q}$ and $\mathbf{j}_s$ from Eqs. (26) and (28) in Eq. (25) we obtain

$$(\rho c)_f \left(\frac{\partial T}{\partial t} + \mathbf{V} \cdot \nabla T \right) = k \nabla^2 T + (\rho c)_s \left(D_B \nabla C \cdot \nabla T + D_T \frac{\nabla T \cdot \nabla T}{T_\infty} \right). \tag{25}$$

The equation for nanoparticle conservation without chemical reaction and dilute mixture can be written as:

$$\frac{\partial C}{\partial t} + \mathbf{V}.\nabla C = -\frac{1}{\rho_s} \nabla . \mathbf{j}_s, \tag{26}$$

which after substituting the expression for $\mathbf{j}_s$ become

$$\frac{\partial C}{\partial t} + \mathbf{V}.\nabla C = \nabla . \left(D_B \nabla C + D_T \frac{\nabla T}{T_\infty} \right). \tag{27}$$

References

1. S. U. S. Choi and J. A. Eastman, Enhancing thermal conductivity of fluids with nanoparticles, in: The Proceedings of the 1995 ASME International Mechanical Engineering Congress and Exposition, San Francisco, USA, ASME, FED 231/MD, 66 (1995) 99–105.
2. O. Mahian, A. Kianifar, S. A. Kalogirou, I. Pop and S. Wongwises, A review of the applications of nanofluids in solar energy, Int. J. Heat Mass Transf. 57 (2013) 582-594.
3. J. Buongiorno and L. W. Hu, Nanofluid heat transfer enhancement for nuclear reactor applications, ASME (Second International Conference on Micro/Nanoscale Heat and Mass Transfer) 3 (2009) 517-522 doi:10.1115/MNHMT2009-18062.
4. K. V. Wong and O. D. Leon, Applications of Nanofluids: Current and Future, Advan. Mech. Engg. 2010 Article ID 519659.
5. R. K. Tiwari and M. K. Das, Heat transfer augmentation in a two-sided lid-driven differentially heated square cavity utilizing nanofluids, Int. J. Heat & Mass Transf. 50 (2007) 2002-2018.
6. J. Buongiorno, Convective transport in nanofluids, ASME J. Heat Transf. 128 (2006) 240–250.
7. A. V. Kuznetsov and D. A. Nield, Natural convective boundary-layer flow of a nanofluid past a vertical plate, Int. J. Therm. Sci. 49 (2010) 243-247.

8. D. A. Nield and A. V. Kuznetsov, The Cheng–Minkowycz problem for natural convective boundary-layer flow in a porous medium saturated by a nanofluid, Int. J. Heat Mass Transf. 52 (2009) 5792-5795.
9. N. Bachok, A. Ishak and I. Pop, Boundary-layer flow of nanofluids over a moving surface in a flowing fluid, Int. J. Thermal Sci. 49 (2010) 1663-1668.
10. W. A. Khan and I. Pop, Boundary-layer flow of a nanofluid past a stretching sheet, Int. J. Heat Mass Transf. 53 (2010) 2477-2483.
11. M. Mustafa, T. Hayat, I. Pop, S. Asghar and S. Obaidat, Stagnation-point flow of a nanofluid towards a stretching sheet, Int. J. Heat Mass Transf. 54 (2011) 5588-5594.
12. A. Aziz and W. A. Khan, Natural convective boundary layer flow of a nanofluid past a convectively heated vertical plate, Int. J. Therm. Sci. 52 (2012) 83-90.
13. M. Mustafa, M. A. Farooq, T. Hayat and A. Alsaedi, Numerical and series solutions for stagnation-point flow of nanofluid over an exponentially stretching sheet, PLoS ONE 8 (2013) doi:10.1371/journal.pone.0061859.
14. M. Mustafa, T. Hayat and A. Alsaedi, Unsteady boundary layer flow of nanofluid past an impulsively stretching sheet, J. Mech. 29 (2013) 423-432.
15. O. D. Makinde, W. A. Khan and Z. H. Khan, Buoyancy effects on MHD stagnation point flow and heat transfer of a nanofluid past a convectively heated stretching/shrinking sheet, Int. J. Heat Mass Transf. 62 (2013) 526-533.
16. M. M. Rashidi, S. Abelman and N. Freidoonimehr, Entropy generation in steady MHD flow due to a rotating porous disk in a nanofluid, Int. J. Heat Mass Transf. 62 (2013) 515-525.
17. M. Turkyilmazoglu, Unsteady convection flow of some nanofluids past a moving vertical plate with heat transfer, ASME J. Heat Transf. 136 (2013) 031704 doi: 10.1115/1.4025730.
18. M. Turkyilmazoglu and I. Pop, Heat and mass transfer of unsteady natural convection flow of some nanofluids past a vertical infinite flat plate with radiation effect, Int. J. Heat Mass Transf. 59 (2013) 167-171.
19. A. V. Kuznetsov and D. A. Nield, Natural convective boundary-layer flow of a nanofluid past a vertical plate: A revised model, Int. J. Therm. Sci. 77 (2014) 126-129.
20. M. Sheikholeslami, M. G. Bandpy, R. Ellahi, M. Hassan, S. Soleimani, Effects of MHD on Cu-water nanofluid flow and heat transfer by means of CVFEM, J. Magn. Magn. Mater. 349 (2014) 188-200.
21. M. Sheikholeslami, M. Gorji-Bandpy, D. D. Ganji and S. Soleimani, Thermal management for free convection of nanofluid using two phase model, J. Mol. Liq. 194 (2014) 179-187.
22. M. M. Rashidi, N. Freidoonimehr, A. Hosseini, O. A. Bég and T. K. Hung, Homotopy simulation of nanofluid dynamics from a non-linearly stretching isothermal permeable sheet with transpiration, Meccan. 49 (2014) 469-482.
23. M. Mustafa, J. A. Khan, T. Hayat and A. Alsaedi, Boundary layer flow of nanofluid over a non-linearly stretching sheet with convective boundary condition, IEEE-Trans. Nanotech. 14 (2015) 159-168.
24. A. Mushtaq, M. Mustafa, T. Hayat and A. Alsaedi, Nonlinear radiative heat transfer in the flow of nanofluid due to solar energy: A numerical study, J. Taiwan Inst. Chem. Eng. 45 (2014) 1176-1183.

25. M. Mustafa, J. A. Khan, T. Hayat and A. Alsaedi, Three-dimensional flow of nanofluid over a non-linearly stretching sheet: An application to solar energy, Int. J. Heat Mass Transf. In Press (2015).
26. M. Mustafa, J. A. Khan, T. Hayat and A. Alsaedi, Analytical and numerical solutions for axisymmetric flow of nanofluid due to non-linearly stretching sheet, Int. J. Non-Linear Mech. 71 (2015) 22-29.
27. M. Mustafa, A. Mushtaq, T. Hayat and B. Ahmad, Nonlinear radiation heat transfer effects in the natural convective boundary layer flow of nanofluid past a vertical plate: A numerical study, PLoS ONE 9 (2014) doi: 10.1371/journal.pone.0103946.
28. J. Harris, Rheology and Non-Newtonian Flow, Longman, London, 1977.
29. K. Sadeghy, A. H. Najafi and M. Saffaripour, Sakiadis flow of an upper-convected Maxwell fluid, Int. J. Nonlinear Mech. 40 (2005) 1220-1228.
30. K. Sadeghy, H. Hajibeygi, S. M. Taghavi, Stagnation point flow of upper-convected Maxwell fluids, Int. J. Non-Linear Mech. 41 (2006) 1242–1247.
31. M. Kumari and G. Nath, Steady mixed convection stagnation-point flow of upper convected Maxwell fluids with magnetic field, Int. J. Nonlinear Mech. 44 (2009) 1048-1055.
32. T. Hayat, Z. Abbas and M. Sajid, MHD stagnation-point flow of an upper-convected Maxwell fluid over a stretching surface, Chaos Solitons and Fractals 39 (2009) 840-848.
33. B. Raftari and A. Yildirim, The application of homotopy perturbation method for MHD flows of UCM fluids above porous stretching sheets, Comp. Math. Appl. 59 (2010) 3328-3337.
34. S. Mukhopadhyay, Heat transfer analysis of the unsteady flow of a Maxwell fluid over a stretching surface in the presence of a heat source/sink, Chin. Phys. Let. 29 (2011) DOI: 10.1088/0256-307X/29/5/054703.
35. T. Hayat, Z. Iqbal, M. Mustafa and A. Alsaedi, Momentum and heat transfer of an upper-convected Maxwell fluid over a moving surface with convective boundary conditions, Nucl. Eng. Des. 252 (2012) 242-247.
36. M. S. Abel, J. V. Tawade and M. M. Nandeppanavar, MHD flow and heat transfer for the upper-convected Maxwell fluid over a stretching sheet, Meccanica 47(2012) 385-393.
37. T. Hayat, M. Mustafa, S. A. Shehzad and S. Obaidat, Melting heat transfer in the stagnation-point flow of an upper-convected Maxwell (UCM) fluid past a stretching sheet, Int. J. Numer. Meth. Fluids 68 (2012) 233-243.
38. S. Shateyi, A new numerical approach to MHD flow of a Maxwell fluid past a vertical stretching sheet in the presence of thermophoresis and chemical reaction, Bound. Val. Prob. 196 (2013) DOI: 10.1186/1687-2770-2013-196.
39. A. Mushtaq, M. Mustafa, T. Hayat and A. Alsaedi, Effect of thermal radiation on the stagnation-point flow of upper-convected Maxwell fluid over a stretching sheet, J. Aerosp. Engg. 27 (2014) 04014015.
40. M. Mustafa, J. A. Khan, T. Hayat and A. Alsaedi, Sakiadis flow of Maxwell fluid considering magnetic field and convective boundary conditions, AIP Advances 5 (2014) doi: 10.1063/1.4907927.
41. R. Cortell, A numerical tackling on Sakiadis flow with thermal radiation, Chin. Phys. Let. 25 (2008) doi:10.1088/0256-307X/25/4/048.
42. J. Harris, Rheology and Non-Newtonian Flow, Longman, London, (1977) p. 28.

43. B. A. Bhanvase, M. R. Sarode, L. A. Putterwar, K. A. Abdullah, M. P. Deosarkar and S. H. Sonawane, Intensification of convective heat transfer in water/ethylene glycol based nanofluids containing TiO 2 nanoparticles, Chemical Engineering and Processing: Process Intensification 82 (2014) 123-131.

Table 1: Numerical values of $\theta'(0)$ for different values of Pr and De when $Sc = 1$ and $Nb = Nt = 0.5$. Parentheses include the corresponding numerical results using *bvp4c*.

*De**Pr*	7	8	9	10	11	12
0	-1.2849805	-1.3809984	-1.4711542	-1.5564065	-1.6374779	-1.7149293
	(-1.2849812)	(-1.3809991)	(-1.4711552)	(-1.5564076)	(-1.6374789)	(-1.7149303)
0.5	-1.2965174	-1.3929259	-1.4833739	-1.5688504	-1.6500977	-1.7276895
	(-1.2965181)	(-1.392927)	(-1.4833753)	(-1.5688517)	(-1.6500992)	(-1.7276908)
1	-1.3091365	-1.4061122	-1.4969613	-1.5827295	-1.664194	-1.7419509
	(-1.3091378)	(-1.4061138)	(-1.4969634)	(-1.5827317)	(-1.6641962)	(-1.7419539)
1.5	-1.3218163	-1.4199434	-1.5115798	-1.5978944	-1.6797436	-1.7577751
	(-1.3218184)	(-1.419945)	(-1.5115827)	(-1.5978975)	(-1.6797469)	(-1.7577784)

Table 2: Numerical values of $\theta'(0)$ for different values of Nt and De when $Pr = 7$, $Sc = 1$ and $Nb = 0.5$. Parentheses include the corresponding numerical results using *bvp4c*.

*De**Nt*	0.1	0.3	0.5	0.7	0.9	1.1
0	-1.3669952	-1.3263597	-1.2849805	-1.2428701	-1.200057	-1.1565938
	(-1.3669996)	(-1.3263621)	(-1.2849812)	(-1.2428689)	(-1.200057)	(-1.1565937)
0.5	-1.3784842	-1.3378808	-1.2965174	-1.254401	-1.2115543	-1.1680176
	(-1.3784892)	(-1.3378833)	(-1.2965181)	(-1.2544001)	(-1.211552)	(-1.1680176)
1	-1.3911641	-1.3505547	-1.3091365	-1.2669296	-1.2239366	-1.1801856
	(-1.3911701)	(-1.3505503)	(-1.3091378)	(-1.266929)	(-1.2239344)	(-1.1801821)
1.5	-1.404419	-1.3635612	-1.3218163	-1.2791572	-1.235565	-1.1910351
	(-1.404425)	(-1.3635653)	(-1.3218184)	(-1.2791575)	(-1.2355642)	(-1.1910325)

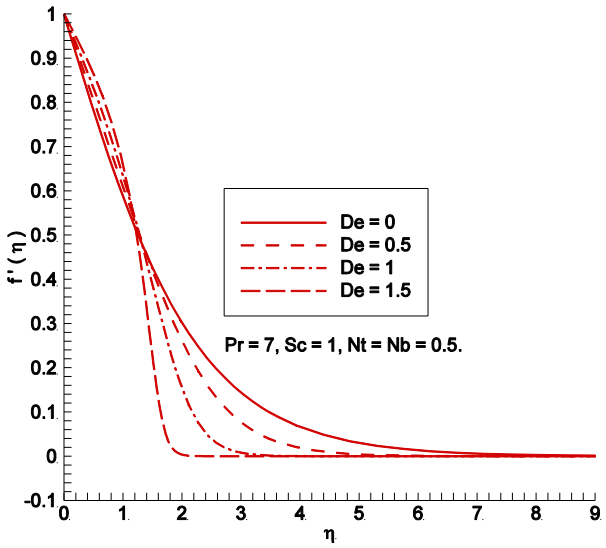

Fig. 2: Effect of De on $f'(\eta)$.

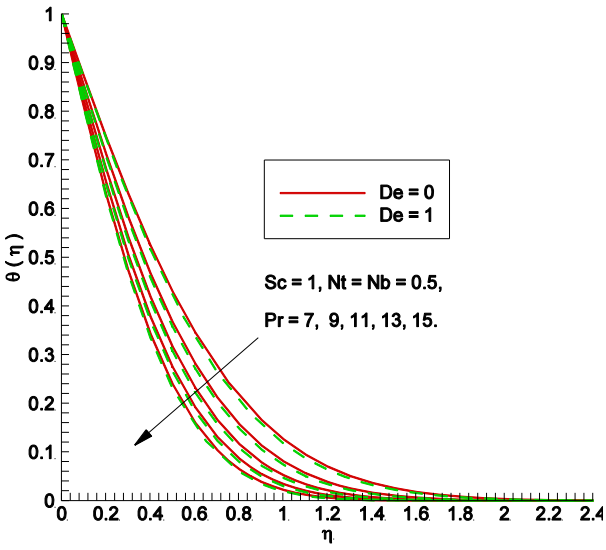

Fig. 3: Effect of Pr on $\theta(\eta)$.

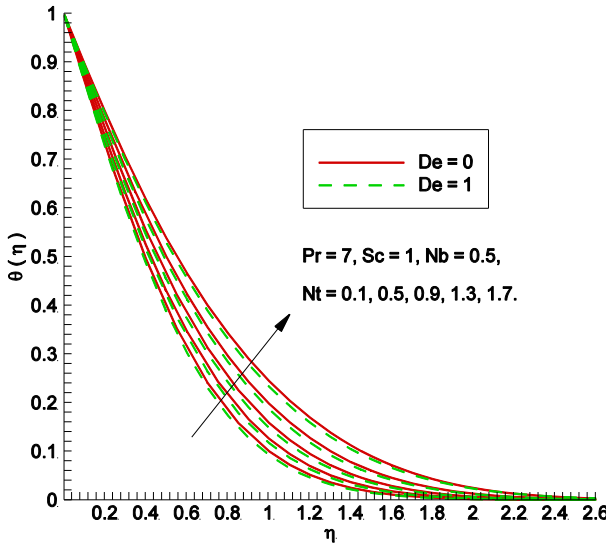

Fig. 4: Effect of Nt on $\theta(\eta)$.

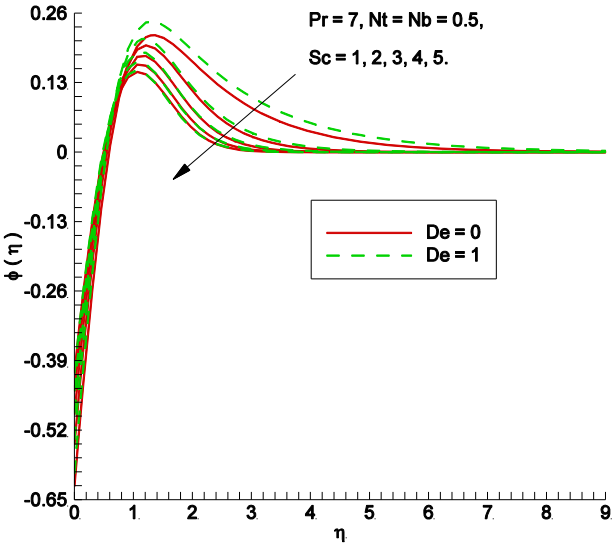

Fig. 5: Effect of Sc on $\phi(\eta)$.

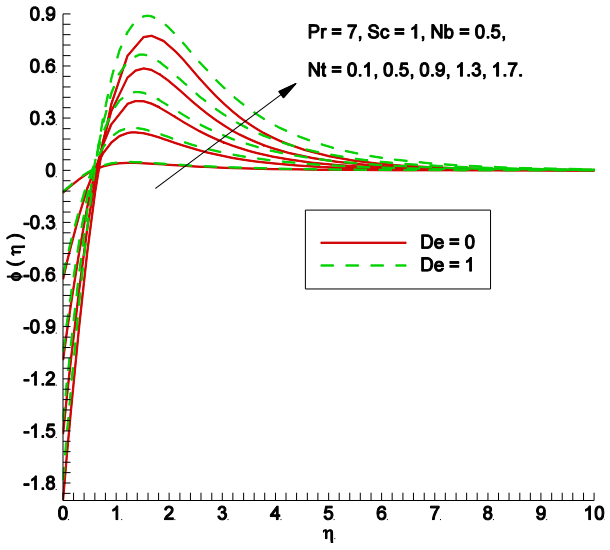

Fig. 6: Effect of Nt on $\phi(\eta)$.

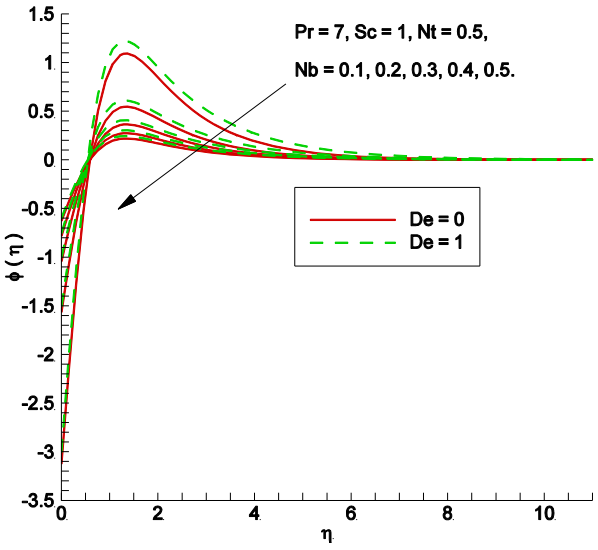

Fig. 7: Effect of Nb on $\phi(\eta)$.

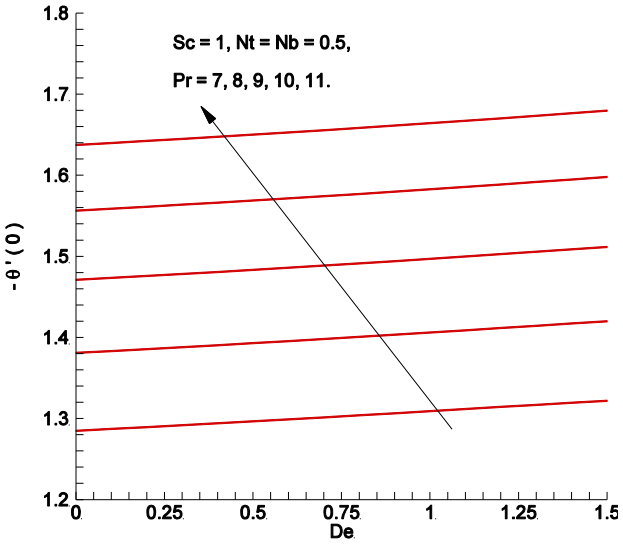

Fig. 8: Effects of Pr and De on $-\theta'(0)$.

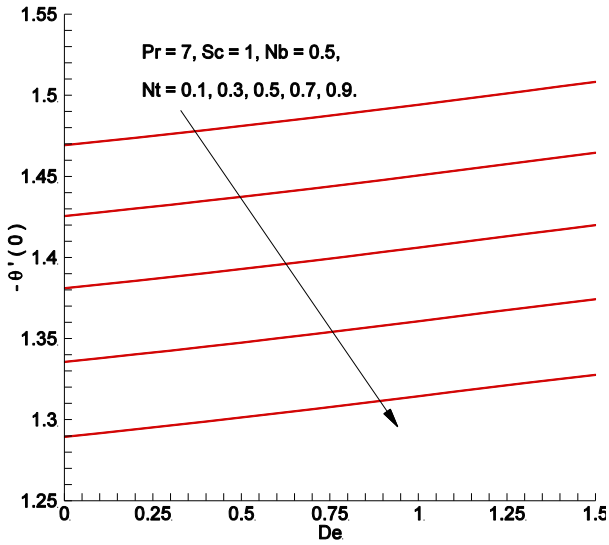

Fig. 9: Effect of Nt on $-\theta'(0)$.